

# SU(2) Colour Fields around Static Sources

G.S. Bali, C. Schlichter and K. Schilling\*

Physics Department, University of Wuppertal, 42097 Wuppertal, Germany

First results of an ongoing high statistics study of the colour flux distribution around static quark sources in  $SU(2)$  gauge theory are presented. The flux tube profiles and widths have been investigated for several quark separations at  $\beta = 2.5$  and  $\beta = 2.74$ . The results are tested against Michael's sum rules.

## 1. INTRODUCTION

Recently, high statistics studies of the static  $q\bar{q}$  potential in  $SU(2)$  and  $SU(3)$  gauge theories have been performed [1]. A linear long range potential with the universal subleading  $-\pi/(12R)$  correction (for quark separations  $Ra > 0.5$  fm), as predicted by the string picture [2], is observed. Moreover, the gap between the ground state potential and the first excited state potential for large  $R$  is consistent with the string value of  $\pi/R$  [3]. The hope for a deeper understanding of the underlying dynamics of the confinement mechanism is one of the motivations for the present investigation. Effective models like a bosonic string model [2], based on a Nielsen-Olesen szenario of magnetic confinement [4] can be tested.

Measurements of colour flux distributions are extremely difficult because the relevant correlators of pure glue quantities exhibit large statistical fluctuations. For this reason, previous studies (e.g. Refs. [5,6]) have only been qualitative. In view of the great progress achieved recently in hardware and lattice techniques (improved operators, noise reduction, updating algorithm), it appears to be of considerable interest to perform really reliable quantitative studies of field distributions. I will report on first results of an ongoing project with this aim.

## 2. SIMULATION

We study lattice volumes of  $16^4$  at  $\beta = 2.5$  ( $a \approx 0.085$  fm) and  $32^4$  at  $\beta = 2.74$  ( $a \approx 0.041$  fm).

\*Work supported by DFG grant Schi 257/1-4 and EC project SC1\*-CT91-0642.

Thus, the physical volumes are  $(1.3 \text{ fm})^4$  in either case. The scale has been extracted from the string tension value  $\sqrt{\sigma} = 440$  MeV. For the updating a hybrid of heatbath and overrelaxation has been used (details in Ref. [7]). Measurements of the relevant operators have been taken every 100 sweeps. At the two  $\beta$  values, 8640 and 670 such statistically independent measurements have been taken, respectively. For safety, the data was binned into blocks of *five* prior to the analysis.

The chromoelectric (and -magnetic) field distributions in presence of two static quarks have been measured for various quark separations  $r = Ra$ . The quarks are generated at time  $t = 0$ , and annihilated at time  $t = Ta$ . This is realized by use of Wilson loops  $W(R, T)$ . A variant of APE smearing [8] has been applied to the spatial parts of the Wilson loops in order to increase the ground state overlaps. All overlaps have been found to be larger than 95% in the potential analysis.

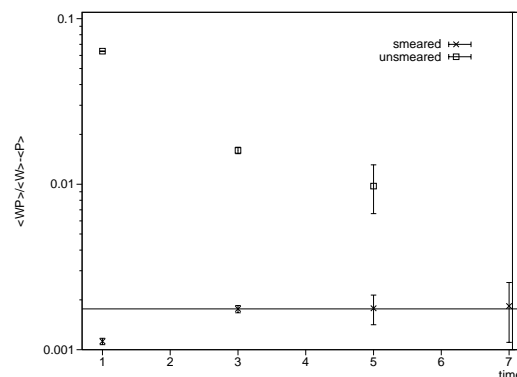


Figure 1. Comparison between smeared and unsmeared operators for  $\varepsilon(\mathbf{0})$  at  $\beta = 2.5$ ,  $R = 4$ .

The Maxwell field strength tensor is given by  $F_{\mu\nu}^a{}^2 = 2\text{Tr}\mathcal{F}_{\mu\nu}^2 \approx 2\beta/a^4 S_{\mu\nu}$  with  $S_{\mu\nu} = 1 - \frac{1}{N}\text{Re Tr}(U_{\mu\nu})$  being the plaquette action. Due to its locality,  $S_{\mu\nu}$  undergoes a multiplicative renormalization which, in the mean field approximation, is cancelled out in the combination  $\beta S_{\mu\nu}$ .

We measure the difference between this operator in presence of the  $q\bar{q}$  pair, separated by a distance  $r$ , and its vacuum expectation for various times  $T$ :

$$P_{\mu\nu}^{(R,T)}(\mathbf{n}) = \frac{\langle W(R,T)S_{\mu\nu}(\mathbf{n}, T/2) \rangle}{\langle W(R,T) \rangle} - \langle S_{\mu\nu} \rangle. \quad (1)$$

The (squared) field components are given by

$$E_{(r)i}{}^2(\mathbf{n}a) = \frac{2\beta}{a^4} P_{i4}^{(R,T)}(\mathbf{n}) \quad , \quad (2)$$

$$B_{(r)i}{}^2(\mathbf{n}a) = \frac{2\beta}{a^4} \epsilon_{ijk} P_{jk}^{(R,T)}(\mathbf{n}) \quad (3)$$

for  $T$  large. From these fields, the energy,  $\varepsilon(\mathbf{x})$ , and action densities,  $\sigma(\mathbf{x})$ , are calculated:

$$\left. \begin{array}{l} \varepsilon_{(r)}(\mathbf{x}) \\ \sigma_{(r)}(\mathbf{x}) \end{array} \right\} = \frac{1}{2} \left( \mathbf{E}_{(r)}^2(\mathbf{x}) \pm \mathbf{B}_{(r)}^2(\mathbf{x}) \right) \quad . \quad (4)$$

Since  $B_i^2 \leq 0$  in the chosen Minkowski notation, the energy densities are very small and, thus, extremely difficult to measure. In the actual simulation, various electric/magnetic plaquettes have been averaged, in order to obtain an operator that is symmetric around the lattice site  $(\mathbf{n}, T/2)$ .

Early investigations have failed to identify the asymptotic plateau (Eqs. (2,3)). This situation is greatly improved by smearing techniques, as can be seen from Fig. 1 where a comparison of  $\varepsilon_{(4a)}(\mathbf{0})$  (at  $\beta = 2.5$ ) from smeared and unsmeared Wilson loops is made. Also, the statistical errors are substantially reduced (note the logarithmic scale). The coordinate system is chosen such that the quark source resides at the spatial coordinate  $(0, 0, R/2)$ , and the antiquark at  $(0, 0, -R/2)$ . The fields have been measured at all points  $\mathbf{n}$  with  $n_3$  being varied along the whole lattice axis, while the transverse distance  $n_\perp = (n_1, n_2)$  is taken along the directions  $(1, 0)$ , and  $(1, 1)$  up to  $|n_\perp| = 6$ .

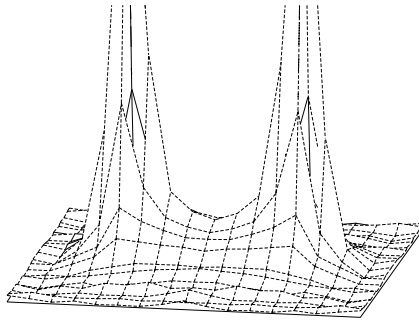


Figure 2. The action density  $\sigma(\mathbf{n})$  at  $\beta = 2.5$ ,  $r = 8a \approx 0.7$  fm.

### 3. RESULTS

In Fig. 2, the measured action density (at  $\beta = 2.5$ ,  $r = 8a \approx 0.7$  fm) is displayed. The resolution of our lattice allows us to see smooth physical structures without any recourse to fancy interpolations. Note that the mesh is not equidistant in the perpendicular direction because the off-axis separations  $n_\perp \propto (1, 1)$  are included.

It is instructive to investigate the field components parallel ( $E_\parallel^2 = E_z^2$ ) and perpendicular ( $E_\perp^2 = E_x^2 + E_y^2$ ) to the flux tube. Around the middle of the confining string ( $\mathbf{n} = 0$ )  $B_\parallel^2 < B_\perp^2 \lesssim E_\perp^2 \ll E_\parallel^2$  is observed. Nice scaling behaviour of the colourfields is found between the two  $\beta$ -values. Within statistical accuracy, continuum rotational invariance is restored.

The energy and action distributions in the central perpendicular plane ( $n_3 = 0$ ) have been investigated. Gaussian fits  $\varepsilon(x_\perp, 0) = c^2 \exp(-x_\perp^2/b^2)$  and dipole fits  $\varepsilon(x_\perp, 0) = c^4/(x_\perp^2 + b^2)^3$  have been performed. In addition, we have numerically integrated the densities within a circle with the cut-off radius  $x_{\max}$

$$I_\varepsilon(f, r) = \int_{x_\perp^2 \leq x_{\max}^2} d^2x_\perp \varepsilon_{(r)}(x_\perp, 0) f(x_\perp) \quad . \quad (5)$$

$x_{\max}$  has been varied in order to identify a plateau. The width is defined by  $\rho_\varepsilon^2(r) = I_\varepsilon(x_\perp^2, r)/I_\varepsilon(1, r)$ . For the above fit functions one obtains  $\rho_\varepsilon^2 = b^2$ . For  $r < 0.4$  fm the dipole fits yield better  $\chi^2$  values. For larger  $q\bar{q}$  separations both  $\chi^2$  turn out to be acceptable but

the Gaussian results are closer to the numerically integrated values. The same holds true for  $\rho_\sigma$ . The electric field  $\mathbf{E}^2(x_\perp, 0)$  is expected to have a Gaussian shape within the confining string [2].

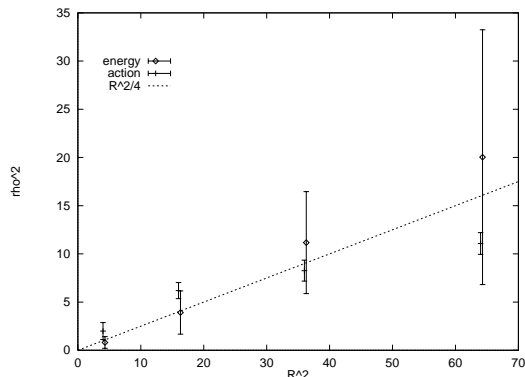


Figure 3. Widths of the energy and action flux tubes  $\rho_{\epsilon/\sigma}^2$  (numerically integrated) as a function of  $R^2$  in lattice units.

$\rho_\epsilon^2$  and  $\rho_\sigma^2$  are plotted against  $R^2$  in Fig. 3. Both, the action, and the energy density widths increase with  $R$ . In the Coulomb-dominated region of the potential ( $R < 0.4$  fm) a dipole behaviour  $\rho_{E^2}^2(R) = R^2/4$  is expected. This straight line is plotted together with the data. For large separations we expect a logarithmic dependence from the string picture [2]. The actual lattice volumes are still too small to investigate this effect.

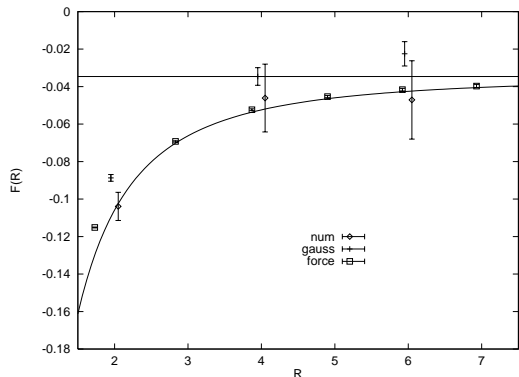


Figure 4. Comparison between the (Gaussian and numerically) integrated perpendicular energy density and the interquark force (Eq. 6).

The integrated energy density should equal the potential between the quarks up to an additive self energy [9] (and the multiplicative field renormalization which is approximately *one* for the lattice field operators chosen). Under the assumption that on increasing the  $q\bar{q}$  separation, the additional binding energy is completely localized near the center of the two the sources (which is expected as soon as an effectively one dimensional string has been formed), a differential form of this sum rule can be derived:

$$F(R) = -a^2 \int d^2 x_\perp \varepsilon_{(Ra)}(x_\perp, 0) \quad , \quad (6)$$

where  $F(R) = -\partial V(R)/\partial R$  is the interquark force (in lattice units). This relation is tested in Fig. 4. Agreement is found even for  $R = 2$ , a distance, where the Coulomb contribution to the potential clearly dominates. This is reflected in an extreme stability of the shapes of the field distributions near the sources against increasing the quark separation.

Till now, we have only realized physical quark separations smaller than 0.7 fm, where a one dimensional string is not yet really formed. Thus, small differences between the fields at  $n_3 = 0$  and  $n_3 = 1$  are still visible. Work on a lattice of linear extent  $L \approx 2.7$  fm is in progress [7].

## REFERENCES

1. G.S. Bali and K. Schilling, Phys. Rev. D47 (1993) 661; UKQCD Collaboration: S.P. Booth et al., Nucl. Phys. B394 (1993) 509.
2. M. Lüscher, G. Münster, and P. Weisz, Nucl. Phys. B180 (1981) 1.
3. C. Michael and S. Perantonis, Nucl. Phys. B347 (1990) 854.
4. H.B. Nielsen and P. Olesen, Nucl. Phys. B61 (1973) 45.
5. R. Sommer, Nucl. Phys. B306 (1988) 181.
6. R.W. Haymaker and J. Wosiek, Phys. Rev. D43 (1991) 2676.
7. C. Schlichter et al., in preparation.
8. The APE Collaboration: M. Albanese et al., Phys. Lett. B192 (1987) 163.
9. C. Michael, Nucl. Phys. B280 (1987) 13.